Pure Appl. Chem., Vol. 77, No. 9, pp. 1595–1605, 2005.
DOI: 10.1351/pac200577091595

Synthetic and computational modeling of the vanadium-dependent haloperoxidases*

Joslyn Yudenfreund Kravitz and Vincent L. Pecoraro‡

Department of Chemistry, University of Michigan, Ann Arbor, MI 48109-1055, USA

Abstract: Vanadium-dependent haloperoxidases that catalyze the halogenation of organic substrates using hydrogen peroxide to oxidize halides are a rare class of enzymes which have an absolute requirement for vanadium. In this article, we describe studies using synthetic, small-molecule analogs of the vanadium(V) active site to functionally mimic the oxidation of bromide and thioethers. In addition, we describe computational studies using density functional theory that help describe the mechanism of catalysis.

Keywords: Vanadium; haloperoxidase; chloroperoxidase; bromoperoxidase; DFT.

INTRODUCTION

Vanadium-dependent haloperoxidases (VHPOs) are enzymes that catalyze the two-electron conversion of halide ions to the corresponding hypohalous acids using hydrogen peroxide as an oxidant [1]:

$$H_2O_2 + H^+ + X^- \rightarrow H_2O + \text{“HOX”} \quad (1)$$

In the presence of a suitable substrate, halogenation of an organic molecule will take place; however, if an appropriate substrate is unavailable, the enzyme will catalyze the disproportionation of hydrogen peroxide at basic pH. Each enzyme is named based on its ability to oxidize halides. The enzyme from *Curvularia inaequalis* is capable of oxidizing chloride, bromide, and iodide and is thus a chloroperoxidase (VClPO). The enzymes from *Ascophyllum nodosom* and *Corallina officianalis* can only oxidize bromide and iodide, not chloride, and are thus bromoperoxidases (VBrPOs). The identity of “HOX” in eq. 1 is dependent upon both the pH of the reaction and the halide involved. Studies indicate that the VClPO oxidizes a chloride ion to HOCl [2], whereas the products of bromide oxidation appear to be a thermodynamic distribution of Br_3^-, HOBr, and Br_2 [3]. In addition to halides, several organic molecules and thioethers can be directly oxidized, with the latter being converted into the corresponding sulfoxide [4].

The VHPOs are found in various fungi and algae. They were first isolated from the brown algae *A. nodosom* in 1983 by Hans Vilter [5]. Heme-based haloperoxidases had been known for some time, but contrary to previously found peroxidases, the enzyme from *A. nodosom* was not inactivated by cyanide [6]; instead, treatment with EDTA led to inactivity [7]. Addition of simple vanadium salts to the deactivated enzyme restored activity, suggesting that the cofactor was a vanadium species. Wever and coworkers soon isolated similar vanadium-dependent enzymes from several other fungi and algae and demonstrated that the cofactor in the active enzyme was, in fact, a vanadium(V) species of unknown structure and protonation state [8].

*Paper based on a presentation at the 4th International Symposium on Chemistry and Biological Chemistry of Vanadium, Szeged, Hungary, 3–5 September 2004. Other presentations are published in this issue, pp. 1497–1640.

‡Corresponding author: E-mail: vlpec@umich.edu

Enzymological, spectroscopic, and model compound studies have combined to shed considerable light on the major catalytic steps in this system. For some time, there has been compelling evidence that the active site contains a single vanadium ion that is in the +5 oxidation state. Reduction of the metal cofactor leads to inactivity, and slow reoxidation kinetics are observed. While once considered a reasonable possibility, there is no evidence that either the V(IV) or V(III) oxidation states are involved in catalysis. This fact clearly distinguishes the class of VHPOs from the more common heme enzymes, which require the formation of the highly oxidized compound I and compound II intermediates during catalysis. Addition of excess molybdate or phosphate, both of which are isostructural to vanadate, to the apoenzyme led to metal binding but did not provide an active enzyme, indicating that the role of the vanadate is more than purely structural [7]. It was thus hypothesized that the vanadate played the role of a Lewis acid, polarizing the peroxide to facilitate reaction [9]. There is general agreement that halide oxidation occurs via a peroxovandatate species generating an oxidized halide species "HOX" which, depending on the specific halide, can be a mixture of HOX, X_3^-, and X_2. It is not clear whether the "HOX" species is released from the enzyme prior to organic halogenation since there is evidence for both eventualities. The fact that the enzyme can in some instances carry out the subsequent halogenation in a regioselective manner [10] indicates that, at least for some organic substrates, the reaction occurs inside the enzyme active site. However, since not all halogenations are regioselective, it is likely that in many cases the reaction occurs off of the enzyme in solution.

The kinetic mechanism is sequential ordered with peroxide binding prior to the halide. In addition, pH rate profiles showed that there is a catalytic proton involved in the reaction and that the vanadate must be protonated in order for peroxide, the actual oxidizing agent, to bind. It appears that the peroxide group is deprotonated at least once upon binding to the vanadium. It has not been determined whether one peroxide oxygen remains protonated or if both oxygens are deprotonated, generating a symmetric, side-on peroxide. In addition, it is also possible that at least one of the peroxide oxygen atoms is involved in a strong H-bond, which could equivalently activate the substrate. The peroxide binding step is followed by attack and oxidation of the halide. Consequently, the location of halide attack, on the protonated or unprotonated oxygen, is not known. Extended X-ray absorption fine structure (EXAFS) studies suggest that the halide does not bind directly to the vanadium during catalysis, but rather directly attacks one of the vanadate oxygen ligands, most likely derived from the peroxide substrate. After oxidation has occurred, the oxidized halogen species ("HOX" in eq. 1) can be released to halogenate an organic substrate.

While the first crystal of the *A. nodosom* enzyme was reported by Vilter and coworkers in 1988 [11], the structure was not solved by this group until 1999 [12]. In the interim, Wever and coworkers solved the crystal structure of the azide-substituted enzyme from the fungus *C. inaequalis* in 1996 [13], the native and peroxide-bound forms in 1997 [14], and several active site mutants in 1999 [15]. The structures solved by Wever indicate a monomeric protein, as opposed to the homo-dimer found by Vilter. In 2000, Littlechild and coworkers solved the crystal structure for the phosphate-substituted dodecomeric enzyme from the red algae *C. officianalis* [16]. All three enzymes have a nearly conserved active site despite the fact that the overall sequence identity between them is less than 25 %. Owing to the focus on the structural data from *C. inaequalis*, in this paper, we will refer to residues as they are numbered in that enzyme. A depiction of the vanadium active site is provided as Fig. 1.

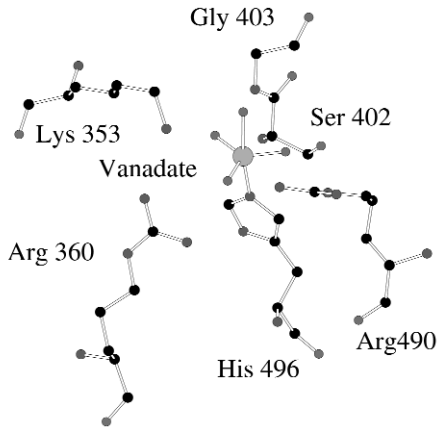

Fig. 1 Active site of the VHPO with residues numbering as in *C. inaequalis* structure [13].

Of all the crystal structures, the *A. nodosom* structure was solved to the highest resolution, at 2.0 Å. The other structures are at resolutions which range up to 2.35 Å. In each structure, the four oxygen atoms of the vanadate group are organized into a trigonal bipyramid in which three of the oxygen atoms form the equatorial plane and one oxygen occupies an axial position. The other axial position is occupied by the nitrogen of a histidine (His496 in the *C. inaequalis* enzyme), which provides the one linkage to the vanadium from the enzyme. Because vanadate has an overall charge of –3, a large amount of charge to be situated in the core of a protein, it has been suggested that the metal cofactor is protonated to some extent in the native state. Additionally, the first shell of residues surrounding the vanadate contain the basic residues Lys353, His404, Arg360, and Arg490. These residues hydrogen-bond to the oxygens, presumably to compensate for the high negative charge of the vanadate and provide stability to the structure, which is essential owing to the lack of covalent interactions between the protein and the cofactor. Mutagenesis studies [15] in which each of these residues, plus His496, were replaced with alanine indicated that His496 and Lys353 are the two most important residues for activity. Replacement of Arg490 or Arg360 leads to a lesser, but still significant, reduction in activity. Additionally, mutation of His404, which is involved in a hydrogen bond with the axial oxygen moiety, or Asp292, which helps orients Arg490 through a strong salt bridge, eliminate almost all activity.

The four basic, hydrogen-bonding residues, in addition to Ser402 and Gly403, which also hydrogen-bond to the cofactor, Asp292 and His496, are all conserved in the two bromoperoxidase structures. In fact, the only large difference between the active site of the VClPO and that of the VBrPOs is the replacement of a phenylalanine in the second shell of the VClPO with a histidine in the VBrPO. It was hypothesized that this change in the active site was responsible for the difference in reactivity between the enzymes, but a recent study by Wever's group, in which the Phe397His mutation was made in the VClPO, resulted in only a partial loss of chloroperoxidase behavior [17]. Thus, there must be longer-range interactions that are responsible for the difference in activity between the forms.

In the peroxo-bound form of the enzyme, whose crystal structure has also been solved by the Wever group, two oxygen atoms from the native form have been replaced by the two oxygens of the peroxide molecule. The trigonal bipyramidal structure of the native enzyme is strongly distorted with one peroxide oxygen occupying the pseudoaxial position trans to His496 and the remaining peroxide oxygen and two vanadate oxygens in the equatorial plane.

Unfortunately, there is little available structural information on the reduced, inactive enzyme form. Both electron paramagnetic resonance (EPR) [9,18] and EXAFS [19] have probed the V(IV) bromoperoxidase. The EPR studies have been particularly enlightening as one can make predictions for the active site using the "additivity relationship". In this technique, the ligands in the equatorial plane of an oxovanadium(IV) species can be determined by evaluating the magnitude of the A_{II} (parallel nu-

clear hyperfine component) in an X-band spectrum. Our group recently assessed the use of the additivity relationship for proteins containing histidine [20,21]. We showed that the orientation of the imidazole influences the magnitude of the contribution of histidine to the value and predicted that there are two histidines bound to the V(IV) in the bromoperoxidase. Subsequent crystallographic analysis of the bromoperoxidase confirmed that this enzyme has an active site more enriched in histidine ligands. These studies may explain why the V(IV) enzyme is inactive and difficult to directly reconstitute.

In contrast to the enzyme crystal structures, all small-molecule model compounds for the VHPOs contain a six-coordinate V(V) atom in both the "native" and peroxo forms. Thus, while these functional model compounds have provided a great deal of information about the catalytic cycle, they tell us little about the structural features of the enzyme. Recently, computational models of the native enzyme and several catalytic intermediates have been used to examine the structural properties of the enzymes. This paper will describe the complementary roles of experimental and theoretical methods to furthering our understanding of these enzymes.

SYNTHETIC MODEL CHEMISTRY

Prior to the solving of the protein's crystal structure, several groups, including ours, synthesized and characterized functional models of the enzyme. These model compounds have been critical for establishing the mechanism of halide and sulfide oxidation by the VHPOs. This paper will focus on studies reported from our group that have provided important insight on this problem.

The first oxoperovanadate species characterized by our group was in 1994 [22] when vanadate and hydrogen peroxide were mixed with *N*-(2-hydroxyethyl)iminodiacetic acid (H_3heida) and a complex capable of brominating phenol red was achieved (Fig. 2). The pentagonal bipyramidal complex contained a side-on bound peroxide in the equatorial plane along with two carboxylates and one imine of the ligand. The axial positions were occupied by an oxo moiety and the alcohol arm of the ligand. UV/vis spectroscopy showed that the oxidation of tetra-*n*-butylammonium bromide to Br^+ with subsequent addition to phenol red, required one equivalent each of hydrogen peroxide and protons (in the form of perchloric acid). In the absence of the phenol red substrate, the complex was found to generate dioxygen upon addition of a second equivalent of hydrogen peroxide and base.

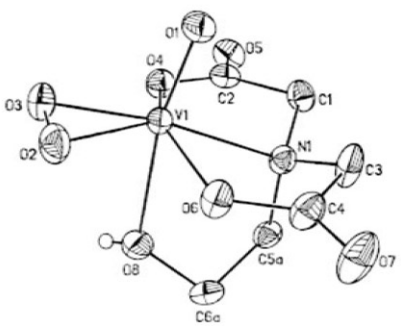

Fig. 2 Crystal structure of $VO(O_2)$heida (obtained from ref. [22]).

In 1996, a series of oxoperoxo species similar to the one described above, was published [23]. Four ligands (Fig. 3), in addition to H_3heida were used in this study: nitrilotriacetic acid (H_3nta), *N*-(2-amidomethyl)iminodiacetic acid (H_2ada), *N,N*-[bis(2-pyridylmethyl]-glycine (Hbpg), and *N,N,N*-tris(2-pyridylmethyl)amine) (tpa). Three new crystal structures were achieved with this ligand set. Upon addition of peroxide and vanadate to H_2ada and Hbpg, crystals suitable for single-crystal X-ray analysis were obtained. The subsequent crystal structures were similar to the previous structures published for the heida and nta complexes. They contained side-on bound peroxide in the equatorial

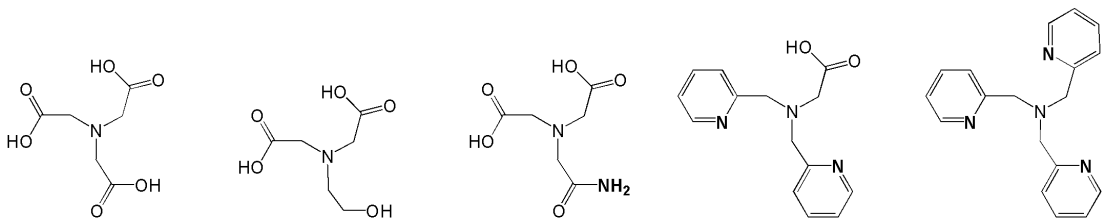

Fig. 3 Ligands used in 1996 study [23].

plane of the pentagonal bipyramidal complexes. In all cases, the central imine of each ligand was coordinated trans to the peroxide and the axial ligand (trans to the oxo moiety) was only weakly coordinated.

Although no crystal structure was obtained for the tpa complex, its reactivity in the presence of acid and halide was investigated along with that of the other complexes. The investigations were carried out in acetonitrile using phenol red as the substrate as before. The reactions were monitored using UV/vis spectroscopy to follow the production of bromphenol blue, the tetrabrominated derivative of phenol red.

The reactivity of these molecules with protons and bromide were explored next. In the absence of bromide, the addition of a proton (in the form of perchloric acid) to these complexes resulted in a subtle, but measurable change in the UV/vis spectra that was interpreted as a protonation of V(V) oxo, peroxo complex. Addition of bromide led to rapid halide oxidation. In contrast, addition of bromide (in the form of tetraethylammonium bromide) to the peroxo complex in the absence of protons resulted in no spectral change, and halide oxidation was not observed. These data were consistent with the initial protonation of the coordinated peroxide to generate the hydroperoxo species, which then would be competent to oxidize bromide. Such a process is in keeping with the ordered kinetic mechanism which requires peroxide to bind before bromide and which shows an essential proton for optimal catalysis. In order to drive the halide oxidation reaction to completion, two equivalents of proton were required—one to protonate the vanadate complex and one to neutralize the hydroxide product. In the presence of substrate, which releases a proton upon bromination, only one additional proton was required for total reaction. The proton dependence of the reaction was found to be pseudo-first-order.

To determine the role of the vanadate in catalysis, the $VO(O_2)$bpg complex was used owing to its solubility in acetonitrile, which is greater than the other complexes used in the study. The role of bromide was studied with all five complexes. The study showed that the reaction was first-order in vanadate as well as in bromide. Further initial rate studies were carried out, and a kinetic model for the reaction was proposed (see Fig. 4).

Although the ligands coordinated to the vanadium in this study are not exactly those found in the enzyme, they are sufficiently similar to allow examination of each step of the catalytic cycle individually, something that is not possible in the protein. In the absence of vanadate complex, peroxide will facilitate the oxidation of bromide, but at a rate which is order of magnitude slower than in the presence of vanadate. Once the peroxide is bound, addition of bromide prior to protonation of the complex leads neither to a change in the UV/vis spectrum of the vanadate complex nor to catalysis, indicating that it is the protonated peroxy species which is catalytically active and binding of bromide to the noncatalytically active species is unlikely.

An analysis of the pK_as of chloride, bromide, and coordinated hydroperoxide provide important insight for the mechanism. In acetonitrile, HBr is more acidic than HCl. Under catalytic turnover conditions, the solution pH is defined by the basicity of the coordinated peroxide and the substrate (either chloride or bromide). The measured pK_a for coordinated hydroperoxide is intermediate between that of

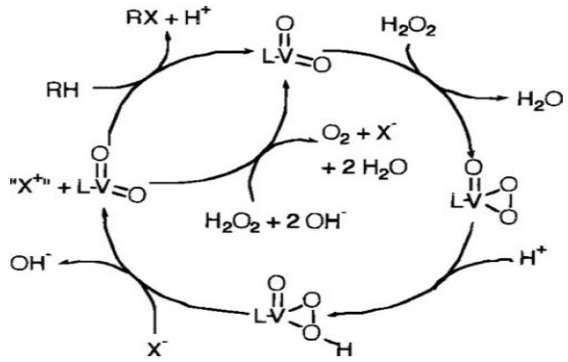

Fig. 4 Proposed catalytic cycle the VHPOs based upon small-molecule model chemistry (adapted from ref. [23]).

HCl and HBr. Therefore, under conditions where the coordinated peroxide can be protonated, the bromide ion will remain unprotonated and susceptible to oxidation. In contrast, the coordinated peroxide is less basic than chloride ion, hence, the hydroperoxide complex can only be prepared after all free chloride has been protonated, which deactiviates the substrate. Hence, these catalysts are only efficient at oxidizing bromide or iodide, but not chloride.

In 1998, the vanadate complexes bpg and ada in the absence of peroxide were synthesized and characterized. A third complex with the ligand *N*-(2-pyridylmethyl)- iminodiacetic acid (H_2pmida) was also characterized [24]. These studies were aimed at determining the kinetics of the first step of the reaction, peroxide binding. This was the one step of the catalytic cycle not examined in the previous study. The reaction was found to be first-order in vanadate at all proton concentration, but first-order in peroxide only in the presence of excess protons.

The proton dependence was found to be very complicated and dependent upon the ratio of protons to vanadate present in solution. While there is a first-order dependence on protons at substoichiometric proton concentrations, in the presence of excess protons, the reaction is insensitive to changes in proton concentration. This is thought to be a result of the reactions being run in acetonitrile since the metal complexes are more basic in this solvent than water. Therefore, the complexes are completely protonated at a stoichiometric proton concentration and the addition of more protons to the solution does not accelerate the reaction. Additionally, the reaction will occur even in the absence of added proton since hydrogen peroxide can act as a proton donor followed by rapid complexation of the peroxide. These experiments indicate that there can be an additional step in the catalytic cycle presented above. That is, the protonation of the resting vanadate species prior to peroxide binding facilitates, but is not essential, to peroxide complexation. As commented upon below in the computational section, it appears that the VHPOs take advantage of this resting-state protonation in order to facilate peroxide binding.

In 2002, our group showed that vanadate complexes of the same ligands that facilitated bromide oxidation could also carry out sulfide oxidation [25]. In addition to being significant from a synthetic perspective, these reactions model the observed oxidation of thioethers to sulfones by VHPOs. One interesting feature of the observed reactivity is that these functional models are capable of rapid oxidation of thioanisole or other substrates to the sulfone, but not to the sulfoxide. This suggests that the thioether substrate undergoes a single oxidation event with the peroxovanadate catalyst. The interpretation of the kinetic mechanism suggests a remarkably similar series of events occur for sulfide oxidation as was observed for halide oxidation. Once again, the peroxovanadate must be protonated for the reaction to occur, and, as expected, protonation of the resting catalyst facilitates peroxide binding. Thus, one could simply substitute dimethyl sulfide or thioanisole for halide in the above reaction scheme and well represent the observed chemistry. The only difference between the two systems is that one equivalent of acid is consumed in each turnover cycle in halide oxidation, whereas sulfide oxidation is catalytic in protons. This is because halide oxidation has hydroxide as a byproduct and sulfide oxidation

has a proton as a byproduct. In fact, excess acid concentrations lead to decomposition of the vanadate complex after turnover. We suspect that the sulfide attacks the hydroperoxovanadate species in a manner that is similar to halide oxidation. It should be noted that chloroperoxidases, unlike bromoperoxidase, have not been reported to catalyze sulfide oxidation.

Small-molecule modeling studies have allowed us to look at the individual steps in the catalytic cycle of the haloperoxidases in a level of detail that is not possible using the protein. From these studies, we have established that protons assist the binding of peroxide to the resting vanadate complex and are essential for the activation of the peroxide once bound to the vanadium. Unfortunately, small-molecule models cannot easily address the precise location of the protonated species necessary for both of these steps. Furthermore, our synthetic models cannot establish whether substrates such as halides or sulfides attack an oxo or hydroxo of the vanadate or whether they react directly with the coordinated peroxide. Because the vanadium oxidation state does not appear to change during the reaction, we have preferred attack at the peroxide; however, these studies do not address whether it is the protonated or unprotonated peroxo oxygen that is attacked and whether the electrophilic peroxo oxygen is in the equatorial or axial position of the vanadate. To address these fundamental questions, we must shift our focus to computational studies.

COMPUTATIONAL MODELING

While synthetic models have shed much light on the reactivity of the vanadate cofactor, they are by no means the only tool at our disposal. In the last decade, computational modeling has become a powerful tool in the field of inorganic chemistry. It not only complements more traditional approaches, but can also address questions that other experiments cannot.

Michael Bühl and coworkers have carried out an extensive series of density functional theory (DFT) calculations in which ^{51}V NMR chemical shift values were calculated [26–29]. His results match very well with experiment and provide the community with another tool for the determination of structure and reactivity of V(V) complexes.

Valeria Conte and coworkers carried out the first computational studies of the catalytic cycle of the VClPO [30]. These calculations, done on very small vanadate models (fewer than ten atoms), provided some insight into the order and location of peroxide and bromide binding and reactivity. One study suggested that an oxo group trans to a nitrogen ligand was unstable and that there is an equilibrium between protonated and nonprotonated peroxide [31]. They showed that side-on binding of the peroxide was preferred over end-on binding in both solution and the gas phase [32]. Studies concerning the brominated intermediate indicated that a hypobromite-like intermediate, in which one peroxo oxygen is protonated and the other is brominated, is quite likely [33]. Because of the speed of the reaction, synthetic model compounds in which both peroxide and bromide are bound are impossible to isolate, but are quite accessible to computational models.

The studies mentioned above, while quite important, all contained vanadium models that were not representative of the vanadate coordination sphere in the enzyme crystal structure. That is, Bühl's studies all involved six-coordinate vanadium complexes, which were consistent with the synthetic model compounds he had studied, and Conte's models mainly had four-coordinate vanadium centers, incorporating only the minimum number of atoms required to model the chemistry of interest. Our goal was to model the actual active site of the enzyme and to characterize the various catalytic intermediates. Thus, we used the vanadate coordinates from the crystal structure of the VClPO as the starting point for our calculations.

Two significant drawbacks of the crystallography of VHPOs are poor resolution and the inability to identify proton positions. The resolution of all the crystal structures of the VClPO and VBrPO containing vanadate are over 2 Å. Since V–O bonds tend to be 1.9 Å or less, we cannot reliably use the crystal structure to determine the precise distances and geometry around the vanadium. Further, since the available models of the enzyme have not assigned the protons at the active site of the enzymes, we

do not know the total charge of the vanadium center. Given these limitations, we undertook a computational study to characterize the exact ligand set of the vanadium and its interactions with the surrounding residues.

We started with the smallest possible model for the vanadate unit—a vanadium atom with three oxo moieties in one plane and an oxo and an ammonia moiety forming a perpendicular axis [34]. Minimization of this overall –3 charged system led to decomposition, indicating that this is not a stable protonation state. Adding one proton, either to an axial oxo (as proposed in the crystal structure) or to an equatorial oxygen, did not stabilize the complex. It was only upon adding a second proton that we achieved a stable conformation. Out of the four possible positions for the second proton, only the configuration in which there were one axial and one equatorial hydroxo groups and two oxos in the equatorial plane was stable. Adding hydrogen-bond donors and acceptors, in the form of ammonia and ammonium molecules, around the complex did not change this behavior. This indicates that the lowest possible charge on the vanadate is –1, not –2 as proposed in the crystal structure.

We then added a third proton to the five possible positions and minimized these structures alone and in the presence of one or two hydrogen-bond partners. We found two stable minima in the neutral case—one in which there are an axial water and one equatorial hydroxo group, and one in which there are an axial hydroxo and two equatorial hydroxo groups. These two configurations were close enough in energy to indicate that they are likely in equilibrium in the enzyme.

Upon addition of a fourth proton, it was found that if there were a neutral molecule, such as ammonia, in the vicinity of the neutral vanadate, the ammonia would be protonated preferentially over the vanadate. Since modeling and in vitro studies both indicate that the first step in the catalytic cycle is protonation of the cofactor, we concluded that the resting state of the vanadate is anionic and the state resulting from the initial protonation is neutral.

Further studies, based on the crystal structure of the peroxo form of the enzyme, have shed light on the reactivity of the cofactor. Starting with the coordinates of the crystal structure, a minimization of the cofactor with zero, one, or two protons have been carried out by Zampella et al [35]. The V–O bond lengths of the minimized structures indicate that the cofactor that has been singly protonated on one of the oxo groups is the most likely representative of the crystal structure.

Substrates, in the form of Br^- and dimethyl sulfoxide (DMSO), were added to the models to investigate the site of substrate attack. Since the vanadium is only five-coordinate, there is an open binding site which could be filled by the substrate. Calculations indicate that this is not the case, which is in good agreement with EXAFS studies [19]. Potential energy barriers were calculated for the attack of each substrate on each of the peroxo oxygens in a variety of protonation states. It was found that protonating the peroxide lowers the barrier to reaction over no protonation of the cofactor or protonation of a nonperoxo oxygen, however, no stable minimum or transition state was found in the cases where the substrate attacked the protonated peroxo oxygen. We found that protonation of either peroxo oxygen leads to polarization of the peroxo bond, with protonation of the equatorial oxygen leading to greater charge separation. This indicates that the most likely configuration of the cofactor during catalysis is one where the equatorial peroxo oxygen, plus one other equatorial oxygen, is protonated, and the substrate attacks the unprotonated, pseudoaxial peroxo oxygen in a S_N2-like fashion as shown in Fig. 5. Identical results were found for dimethyl sulfide oxidation to the corresponding sulfone.

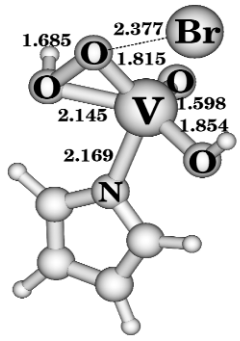

Fig. 5 Attack of halide on the unprotonated, pseudoaxial peroxide oxygen atom [35].

Finally, the role of Lys353 was investigated by including a methyl-ammonium molecule in the vicinity of the equatorial peroxo oxygen, as is found in the crystal structure. This study showed that the barrier to reaction was lowered in the presence of the charged group which polarized the peroxo bond without direct protonation of the peroxide. In fact, in the case of DMSO, the peroxide is not protonated in the transition state. In the case of Br^-, a proton is transferred from the lysine mimic to the peroxide in the transition state. This difference may be attributed the charge on the bromide in the latter case, however, further calculations including counterions showed the same behavior, indicating that this may not be just an artifact of charge separation.

The calculations including counterions indicate that the environment of the active site may be buffering the interaction between Lys353, vanadate, and substrate. To further investigate this, we have undertaken a hybrid quantum mechanics/molecular mechanics (QM/MM) study of the VClPO. Preliminary results [36] from this study indicate the resting state is indeed anionic and that there is a strong hydrogen bond (but no proton transfer) between Lys353 and the vanadate. Furthermore, the vanadate is protonated at one of two other sites.

CONCLUSIONS

It is time to evaluate globally the contributions of the synthetic and computational models of the VHPOs. Our synthetic modeling studies demonstrated that protonation of the coordinated oxo moieties of the vanadate cofactor assists the binding of peroxide. In addition, reactivity studies have shown that protonation of bound peroxide is *essential* for activation of the oxidant in this reaction. Our computational studies have confirmed both of these experimental observations and have provided greater insight into the mechanism. We now realize that the likely site for protonation of the resting state is at both the axial oxygen and one of the equatorial oxygen atoms. This doubly protonated state serves to stabilize the coordinated histidine, which would be unstable trans to a strong π-bonding oxo ligand, while facilitating the loss of an equatorial water upon peroxide complexation. In the catalytically active peroxide state, protonation seems to occur at an equatorial position. There is no evidence that halide binds to the vanadium during the catalytic cycle, and our calculations confirm this observation. Furthermore, we now know that it is the pseudoaxial, unprotonated oxygen of the bound peroxide that is the site of attack by either halides or substrates such as dimethyl sulfide. All of these observations can now be summarized in Fig. 6. It is our belief that the vanadium haloperoxidases represent the ultimate example of how the integration of enzymatic, small-molecule and computational studies allow scientists to establish the mechanism of biochemical catalysis to full chemical resolution. Future studies will focus on understanding what factors differentiate chloro- versus bromoperoxidase activities in these fascinating systems.

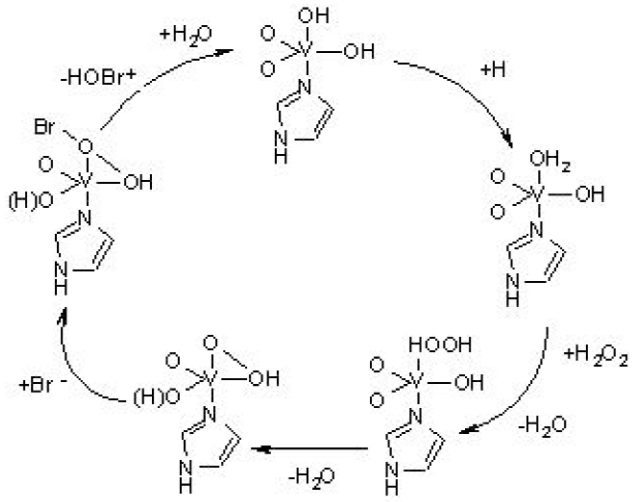

Fig. 6 Our present model for haloperoxidase reactivity. H atoms in parentheses are contributed by hydrogen bond donating ligands.

ACKNOWLEDGMENTS

The authors would like to acknowledge our collaborators, Heather Carlson (College of Pharmacy, University of Michigan) and Luca De Gioia, Guiseppe Zampella, and Piercarlo Fantucci (Department of Biotechnology and Biosciences, University of Milano-Bicocca). Additionally, the authors wish to thank the following funding agencies for support of this work: NIH GM 42703 (VLP) and NIH GM008270 Michigan Molecular Biophysics Training Grant (JYK).

REFERENCES

1. R. R. Everett and A. Butler. *Inorg. Chem.* **28**, 393–395 (1989).
2. J. W. P. M. van Schijndel, P. Barnett, J. Roelse, E. G. M. Vollenbroek, R. Wever. *Eur. J. Biochem.* **225**, 151–157(1994).
3. A. Butler. *Coord. Chem. Rev.* **187**, 17–35 (1999).
4. H. B. ten Brink, A. Tuynman, H. L. Dekker, W. Hemrika, Y. Izumi, T. Oshiro, H. E. Schoemaker, R. Wever. *Inorg. Chem.* **37**, 6780–6784 (1998).
5. H. Vilter, K.-W. Glombitza, A. Grawe. *Botanica Marina* **26**, 331–340 (1983).
6. H. Vilter. *Botanica Marina* **26**, 429–435 (1983).
7. H. Vilter. *Phytochemistry* **23**, 1387–1390 (1984).
8. R. Wever, M. G. M. Tromp, B. E. Krenn, A. Marjani, M. Van Tol. *Environ. Sci. Technol.* **25**, 446–449 (1991).
9. E. de Boer, K. Boon, R. Wever. *Biochemistry* **27**, 1629–1635 (1988).
10. J. S. Martinez, G. L. Carrol, R. A. Tschirret-Guth, G. Altenhoff, R. D. Little, A. Butler. *J. Am. Chem. Soc.* **123**, 3289–3294 (2001).
11. A. Muller-Fahrnow, W. Hinrichs, W. Saenger, H. Vilter. *FEBS Lett.* **239**, 292–294 (1988).
12. M. Weyand, H.-J. Hecht, M. Kie, M.-F. Liaud, H. Vilter, D. Schomburg. *J. Mol. Biol.* **293**, 595–611 (1999).
13. A. Messerschmidt and R. Wever. *Proc. Natl. Acad. Sci. USA* **93**, 392–396 (1996).
14. A. Messerschmidt, L. Prade, R. Wever. *Biol. Chem.* **378**, 309–315 (1997).
15. W. Hemrika, R. Renirie, S. Macedo-Ribeiro, A. Messerschmidt, R. Wever. *J. Biol. Chem.* **274**, 23820–23827 (1999).

16. M. N. Isupov, A. R. Dalby, A. A. Brindley, Y. Izumi, T. Tanabe, G. N. Murshudov, J. A. Littlechild. *J. Mol. Biol.* **299**, 1035–1049 (2000).
17. N. Tanaka, Z. Hasan, R. Wever. *Inorg. Chim. Acta* **356**, 288–296 (2003).
18. E. de Boer, M. G. M. Tromp, H. Plat, G. E. Krenn, R. Wever. *Biochim. Biophys. Acta* **872**, 104–115 (1986).
19. H. Dau, J. Dittmer, M. Epple, J. Hanss, E. Kiss, D. Rehder, C. Schulzke, H. Vilter. *FEBS Lett.* **47**, 237–240 (1999).
20. T. S. Smith, II, J. W. Kampf, P. G. Rasmussen, V. L. Pecoraro. *J. Am. Chem. Soc.* **122**, 767–775 (2000).
21. T. S. Smith II, R. LoBrutto, V. L. Pecoraro. *Coord. Chem. Rev.* **228**, 1–18 (2002).
22. G. J. Colpas, B. J. Hamstra, J. W. Kampf, V. L. Pecoraro. *J. Am. Chem. Soc.* **116**, 3627–3628 (1994).
23. G. J. Colpas, B. J. Hamstra, J. W. Kampf, V. L. Pecoraro. *J. Am. Chem. Soc.* **118**, 3469–3478 (1996).
24. B. J. Hamstra, G. J. Colpas, V. L. Pecoraro. *Inorg. Chem.* **37**, 949–955 (1998).
25. T. S. Smith II and V. L. Pecoraro. *Inorg. Chem.* **41**, 6754–6760 (2002).
26. M. Buhl. *Angew. Chem., Int. Ed*. **37**, 142–144 (1998).
27. M. Buhl. *J. Comp. Chem.* **20**, 1254–1261 (1999).
28. M. Buhl and F. A. Hamprecht. *J. Comp. Chem.* **19**, 113–122 (1998).
29. M. Buhl and M. Parrinello. *Chem. Eur. J.* **7**, 4487–4494 (2001).
30. V. Conte, F. Di Furia, S. Moro, S. Rabbolini. *J. Mol. Cat. A* **113**, 175–184 (1996).
31. V. Conte, O. Bortolini, S. Carraro, S. Moro. *J. Inorg. Biochem.* **80**, 41–49 (2000).
32. V. Conte, F. Di Furia, S. Moro. *J. Mol. Cat. A* **120**, 93–99 (1997).
33. O. Bortolini, M. Carraro, V. Conte, S. Moro. *Eur. J. Biochem.* 42–46 (2003).
34. G. Zampella, J. Y. Kravitz, C. E. Webster, P. Fantucci, M. B. Hall, H. A. Carlson, V. L. Pecoraro, L. De Gioia. *Inorg. Chem.* **43**, 4127–4136 (2004).
35. G. Zampella, P. Fantucci, V. L. Pecoraro, L. De Gioia. *J. Am. Chem. Soc.* **127** (3), 953–960 (2005).
36. J. Yudenfreund Kravitz, V. L. Pecoraro, H. A. Carlson. *J. Chem. Theory Comput.* Accepted for publication.